PHYSICAL REVIEW A VOLUME 55, NUMBER 1 JANUARY 1997

Energy levels of the ground state and the $2s2p$ $(J=1)$ excited states of berylliumlike ions: A large-scale, relativistic configuration-interaction calculation

M. H. Chen and K. T. Cheng
University of California, Lawrence Livermore National Laboratory, Livermore, California 94550

(Received 24 May 1996)

We have calculated energy levels of the $2s^2\ ^1S_0$ ground state and the $2s2p\ ^{1,3}P_1$ excited states of berylliumlike ions with $Z=10$–92 using the relativistic configuration-interaction method. These calculations are based on the relativistic no-pair Hamiltonian which includes Coulomb and retarded Breit interactions and employ finite B-spline basis functions. Quantum electrodynamic and mass polarization corrections are also calculated. Good agreement between theory and experiment for the $2s^2\ ^1S_0-2s2p\ ^{1,3}P_1$ transition energies is found throughout the isoelectronic sequence. [S1050-2947(97)00601-X]

PACS number(s): 31.10.+z, 31.25.−v, 31.30.Jv, 32.30.−r

I. INTRODUCTION

At present, electron correlations and quantum electrodynamic (QED) corrections are the two main uncertainties in *ab initio* atomic structure calculations for highly charged ions. To achieve high accuracy in energy-level calculations, both problems have to be addressed. In recent years, precision experiments on high-Z ions [1–5] have been carried out to test atomic structure theories in strong fields. On the theoretical front, substantial progress has been made in calculating electron correlations and QED corrections in recent years, and several highly accurate calculations of the energy levels of He-like to Na-like ions [6–13] have appeared in the literature.

There exist many relativistic calculations on the energy levels of Be-like ions in the literature. These calculations can be classified into two broad categories: One type of calculation uses nonrelativistic theories to obtain accurate correlation energies and includes relativistic corrections as first-order perturbations [14–18]. The other type of calculation treats electron correlation and relativity on an equal footing. Examples are the multiconfiguration Dirac-Fock (MCDF) method and the relativistic many-body perturbation theory (MBPT). The MCDF method was employed by Cheng, Kim, and Desclaux to calculate the $n=2$ low-lying states for ions in the Li to F isoelectronic sequences [19]. It was also used by Ynnerman and Froese Fischer to study the $2s^2\ ^1S_0-2s2p\ ^{1,3}P_1$ transitions in Be-like ions [20]. Relativistic MBPT calculations were carried out by Liu and Kelly [21] for the ground state of neutral beryllium, and an all-order method was used by Lindroth and Hvarfner [22] for the $2s^2\ ^1S_0$ and $2s2p\ ^{1,3}P_1$ states of Fe^{22+} and Mo^{38+}. Recently, a systematic MBPT calculation including up to second-order contributions for the $n=2$ states of Be-like ions with $Z=4$–100 was reported by Safronova, Johnson, and Safronova [23]. In general, agreements between theory and experiment are good for Be-like ions. However, there is as yet no single theory which can yield highly accurate transition energies along the entire isoelectronic sequence.

In this paper we report a relativistic configuration-interaction (CI) calculation of the $2s^2\ ^1S_0$ ground state and the $2s2p\ ^{1,3}P_1$ excited states of Be-like ions with $Z=10$–92. This method is based on the no-pair Hamiltonian [24,25] and uses B-spline basis functions which are solutions of the radial Dirac equation for an electron moving in a potential confined to a finite cavity [26]. These B-spline orbitals form a complete set of finite, discrete basis functions, and are suitable for high-precision calculations as demonstrated in previous relativistic CI [6–9] and MBPT calculations [10–13]. In this work, CI energies are combined with *ab initio* QED and mass polarization corrections to obtain the total energies. Our present results on the $2s^2\ ^1S_0-2s2p\ ^{1,3}P_1$ transition energies agree quite well with experiment throughout the Periodic Table.

II. THEORETICAL METHOD

Details of our theoretical method have been presented in Refs. [6–8]. Briefly, the relativistic no-pair Hamiltonian for an N-electron system is given by [24,25]

$$H=\sum_{i=1}^{N} h_0(i)+\Lambda_{++}(H_C+H_B)\Lambda_{++}, \tag{1}$$

where h_0 is the single-particle Dirac Hamiltonian for an electron moving in a nuclear Coulomb potential represented by a two-parameter Fermi charge distribution of the nucleus, Λ_{++} is the positive-energy projection operator, and H_C and H_B are the Coulomb and retarded Breit interactions, respectively. The eigenfunction $\Psi(JM)$ of an atomic state with angular momentum (J,M) and parity π is expressed as a linear combination of the many-electron configuration-state functions $\phi(\Gamma_K JM)$:

$$\Psi(JM)=\sum_K c_K\phi(\Gamma_K JM), \tag{2}$$

where Γ_K is a set of quantum numbers representing different electronic configurations, and c_K is the mixing coefficient. Variation of the energy functional $\langle\Psi|H|\Psi\rangle$ with respect to c_K, subjected to the wave-function normalization condition, leads to the CI equation

$$\sum_{L} (H_{KL}-\lambda\,\delta_{KL})c_L=0. \tag{3}$$

Expressions for the matrix elements H_{KL} in terms of the configuration-state functions are given in Ref. [8].

III. NUMERICAL CALCULATIONS

A. Relativistic *B*-spline basis functions

B-spline basis functions for a Dirac electron moving in a model potential confined to a finite cavity are obtained using the method by Johnson, Blundell, and Sapirstein [26]. Model potentials used here are Dirac-Slater (DS) potentials with Kohn-Sham exchanges for the $2s^2$ ground state of Be-like ions. Parameters for the Fermi charge distribution of the nucleus are taken from Johnson and Soff [27], except for thorium and uranium, which are from Zumbro and coworkers [28,29]. The choice of potentials is found to be immaterial here, as we have saturated our CI calculations with all dominant configurations. As for cavity radii, they are chosen so that eigenenergies of the first few s and p states agree precisely with the actual eigenenergies of the unconstrained DS potential. Within reason, the choice of cavity radii is not critical.

In this work, a radius of 8 a.u. is used for neon and a 1/*Z* scaling rule is used to determine the cavity radii of other ions. Also, 30 positive-energy *B*-spline orbitals are generated for each of the $s, p, d, \ldots$ states inside the cavity. We include orbitals with $\ell=0$–5, and use the first 20 orbitals for each of the angular symmetries in our calculations. Contributions from the remaining *B*-spline orbitals are found to be quite negligible.

B. Configuration-state functions

In our basic CI expansion, configuration-state functions (CSF's) include states arising from single and double excitations from the reference states $1s^2 2s^2 + 1s^2 2p^2 \ (J=0)$ and $1s^2 2s2p \ (J=1)$. These CSF's consist of the following configurations:

$$\begin{aligned} 2s^2\ {}^1S_0:&\quad 1s^2 n\ell n'\ell',\quad 1s2sn\ell n'\ell',\quad 1s2pn\ell n'\ell',\\ &\quad 2s^2 n\ell n'\ell',\quad 2p^2 n\ell n'\ell',\\ 2s2p\ {}^{1,3}P_1:&\quad 1s^2 n\ell n'\ell',\quad 1s2sn\ell n'\ell',\\ &\quad 1s2pn\ell n'\ell',\quad 2s2pn\ell n'\ell'. \end{aligned}$$

As the same CSF's can arise from different groups of excitations (e.g., $1s2s2pn\ell$ from $1s2sn\ell n'\ell'$ are the same as $1s2p2sn\ell$ from $1s2pn\ell n'\ell'$), care is taken to ensure that there are no ''double countings'' of CSF's throughout this work.

To carry out CI calculations with $\ell=0$–5, the number of CSF's from single and double excitations can become prohibitively large, especially for the ${}^{1,3}P_1$ states. To make the problem more tractable, we first limit the value of ℓ' to $\ell'=\ell,\ \ell\pm1$. Contributions from CSF's with $\Delta\ell=|\ell-\ell'|\geqslant2$ are small, and are dominated by $nsn'd$ excitations, e.g., $1s2snsn'd$. For the ${}^1S_0$ ground state, we further restrict the $2p^2 n\ell n'\ell$ configurations to those that leave the two excited electrons coupled to an intermediate angular momentum of $J_i=0$, i.e., $n\ell n'\ell[J_i=0]2p^2$. This corresponds to double excitations of the two $1s$ electrons from the $1s^2 2p^2 \ (J=0)$ reference state which preserve the $1s^2$ core angular momentum. Similar restriction is also applied to the $2s2pn\ell n'\ell$ configurations for the ${}^{1,3}P_1$ excited states. Our basic CI calculations thus consist of the following sets of CSF's:

$$\begin{aligned} 2s^2\ {}^1S_0:&\quad 1s^2 n\ell n'\ell,\quad 1s2sn\ell n'\ell,\\ &\quad 1s2pn\ell n'(\ell+1),\\ &\quad 2s^2 n\ell n'\ell,\quad n\ell n'\ell[0]2p^2,\\ 2s2p\ {}^{1,3}P_1:&\quad 1s^2 n\ell n'(\ell+1),\quad 1s2sn\ell n'(\ell+1),\\ &\quad 1s2pn\ell n'\ell,\quad n\ell n'\ell[0]2s2p. \end{aligned}$$

Contributions from $\Delta\ell\geqslant2$ configurations and those from core angular momentum-changing excitations, $n\ell n'\ell'[J_i>0]2p^2 \ (J=0)$ and $n\ell n'\ell'[J_i>0]2s2p \ (J=1)$, are found to be quite small. They are obtained by taking the difference between results of the basic CI calculations with those of two additional calculations: One includes $\Delta\ell\geqslant2$ configurations along with the basic sets of CSF's, and the other includes all possible CSF's from $2p^2 n\ell n'\ell$ for the ${}^1S_0$ ground state and $2s2pn\ell n'\ell$ for the ${}^{1,3}P_1$ excited states. These additional calculations are carried out with $\ell\leqslant3$ orbitals only, as contributions from higher-ℓ states are completely negligible.

In addition to single and double excitations, there are small corrections from triple excitations to the correlation energy. Dominant triple excitation contributions come from $2s2pn\ell n'\ell'$ for the ${}^1S_0$ ground state and from $2s^2 n\ell n'\ell'$ and $2p^2 n\ell n'\ell'$ for the ${}^{1,3}P_1$ excited states. In both cases, we further include contributions from $1s3\ell_b n\ell n'\ell'$, $2\ell_a 3\ell_b n\ell n'\ell'$, $1s4\ell_b n\ell n'\ell'$, and $2\ell_a 4\ell_b n\ell n'\ell'$, where $2\ell_a=(2s,2p)$, $3\ell_b=(3s,3p,3d)$, and $4\ell_b=(4s,4p,4d)$. Here $n, n'\geqslant3$, and calculations are carried out with $\ell, \ell'\leqslant2$ only, as high-ℓ contributions from triple excitations are quite insignificant. These corrections are calculated using CI expansions that includes CSF's from one of these groups of three-electron excitations in addition to two-electron excitations and by subtracting results of similar CI calculations with two-electron excitations only. Test calculations show that quadruple excitations from $3\ell_b 3\ell_b' n\ell n'\ell'$ should contribute less than 10^{-5} a.u. to the correlation energy of Ne^{6+}. Contributions from other triple and quadruple excitations should be negligible.

C. Evaluation of the Hamiltonian matrix

For large-scale computations like the present CI, it is important to organize the calculation as efficiently as possible. In this work, matrix elements are classified according to angular momentum channels. Angular coefficients are evaluated for distinct recoupling channels only and are saved in look-up tables. Also, similar CSF's which share the same Hartree *Y* functions are grouped together to minimize the

TABLE I. CI energies (a.u.) for Be-like neon ($Z=10$) as computed with the four-electron Dirac-Slater potential. Basic, core-ch, $\Delta\ell\geq 2$, and triple are contributions to the Coulomb energy, and no-pair is the sum of the Coulomb and Breit energies. The values listed in the second through fifth rows under each state are increments of energy by adding configurations with successive ℓ symmetries, and ℓ tails are residual high-ℓ contributions.

	Basic	Core-ch	$\Delta\ell\geq 2$	Triple	Coulomb	Breit	No-pair
$2s^2\ ^1S_0$							
sp	−110.425 61	0.000 00		−0.000 01	−110.425 63	0.012 62	−110.413 01
Δd	−0.006 31	−0.000 02	0.000 00	−0.000 01	−0.006 34	−0.000 18	−0.006 52
Δf	−0.001 62	0.000 00	0.000 00		−0.001 62	−0.000 08	−0.001 69
Δg	−0.000 58				−0.000 58	−0.000 04	−0.000 62
Δh	−0.000 26				−0.000 26	−0.000 03	−0.000 28
ℓ tail	−0.000 35				−0.000 35	−0.000 09	−0.000 44
total	−110.434 73	−0.000 02	0.000 00	−0.000 02	−110.434 77	0.012 21	−110.422 56
$2s2p\ ^3P_1$							
sp	−109.906 94	−0.000 48		−0.000 01	−109.907 43	0.012 95	−109.894 47
Δd	−0.013 52	−0.001 43	−0.000 01	−0.000 03	−0.014 98	−0.000 22	−0.015 20
Δf	−0.002 00	0.000 02	0.000 00		−0.001 98	−0.000 08	−0.002 06
Δg	−0.000 59				−0.000 59	−0.000 04	−0.000 63
Δh	−0.000 24				−0.000 24	−0.000 02	−0.000 26
ℓ tail	−0.000 26				−0.000 26	−0.000 08	−0.000 34
total	−109.923 55	−0.001 89	−0.000 01	−0.000 03	−109.925 49	0.012 52	−109.912 97
$2s2p\ ^1P_1$							
sp	−109.390 72	−0.001 19		−0.000 02	−109.391 93	0.012 74	−109.379 19
Δd	−0.051 68	−0.001 47	−0.000 05	−0.000 22	−0.053 42	−0.000 24	−0.053 66
Δf	−0.006 06	0.000 02	0.000 00		−0.006 04	−0.000 08	−0.006 12
Δg	−0.001 76				−0.001 76	−0.000 04	−0.001 80
Δh	−0.000 70				−0.000 70	−0.000 02	−0.000 72
ℓ tail	−0.000 73				−0.000 73	−0.000 08	−0.000 81
total	−109.451 65	−0.002 64	−0.000 05	−0.000 24	−109.454 57	0.012 27	−109.442 30

recomputation of these indefinite integrals. The calculations of full frequency-dependent magnetic and retardation corrections are very time consuming. To reduce the computational effort, off-diagonal matrix elements are evaluated with the unretarded Breit operator, while diagonal matrix elements are calculated with the retarded Breit operator to obtain the leading frequency-dependent corrections to the Breit energies. As evident in the cases of Li-like ions [8] and few-electron uranium ions [9], the effects of neglecting retardation in off-diagonal Breit matrix elements on transition energies are expected to be very small.

The dimensions of the dense, real, symmetric matrices encountered in our present CI calculations range from 10 000 to 36 000. In double-precision, symmetric storage mode, they can reach over five gigabytes in size, and have to be kept as sequential files on on-line hard disks. An iterative Davidson's method [30] as implemented by Stathopoulos and Froese Fischer [31] is used to solve for the first few eigenvalues of the CI equation. Davidson's method is very efficient for our CI matrices, which are diagonally dominated. Typically, only 6–10 iterations are needed in our calculations to achieve convergence.

D. Quantum electrodynamic corrections

In this work, one-electron self-energies are calculated using the scheme of Cheng, Johnson, and Sapirstein [32]. The effects of screening and nuclear finite size are included by using the same model potential as in the CI calculations, namely, Dirac-Slater (DS) potentials with Kohn-Sham exchanges and Fermi nuclear charge distributions for the $2s^2$ ground state of Be-like ions. Leading vacuum polarization corrections are evaluated as expectation values of the Uehling potential using the same DS wave functions. Wichmann-Kroll corrections to the vacuum polarization are taken from the tabulation by Johnson and Soff [27], adjusted by screening factors. Total QED correction for a many-electron eigenstate is given by the sum of the single-particle QED corrections, weighted by the fractional occupation number of each orbital as obtained from the eigenvector of the CI calculation.

IV. RESULTS AND DISCUSSION

Typical results from our calculations are shown in Table I for the $2s^2\ ^1S_0$ ground state and the $2s2p\ ^{1,3}P_1$ excited states of Ne^{6+}. In the second column of this table, we show under ''basic'' Coulomb energies computed with the basic sets of CSF's. The next three columns show contributions to Coulomb energies from core angular momentum-changing corrections ''core-ch,'' from $\Delta\ell=|\ell-\ell'|\geq 2$ configurations ''$\Delta\ell\geq 2$,'' and from triple excitations ''triple.'' These corrections are discussed in Sec. III B. The sums of these four terms give the total Coulomb energies in the sixth column. Total Breit energies are shown in the seventh column.

TABLE II. CI energies (a.u.) for Be-like neon ($Z=10$) as computed with the two-electron Dirac-Hartree potential. Explanations are the same as those in Table I.

	Basic	Core-ch	$\Delta\ell\geqslant 2$	Triple	Coulomb	Breit	No-pair
$2s^2\ ^1S_0$							
sp	−110.425 58	−0.000 01		−0.000 06	−110.425 65	0.012 62	−110.413 03
Δd	−0.006 29	−0.000 02	0.000 00	−0.000 01	−0.006 32	−0.000 18	−0.006 50
Δf	−0.001 61	0.000 00	0.000 00		−0.001 61	−0.000 08	−0.001 69
Δg	−0.000 58				−0.000 58	−0.000 04	−0.000 63
Δh	−0.000 26				−0.000 26	−0.000 03	−0.000 28
ℓ tail	−0.000 35				−0.000 35	−0.000 10	−0.000 45
total	−110.434 67	−0.000 03	0.000 00	−0.000 07	−110.434 77	0.012 20	−110.422 57
$2s2p\ ^3P_1$							
sp	−109.906 91	−0.000 48		−0.000 04	−109.907 43	0.012 96	−109.894 47
Δd	−0.013 30	−0.001 57	−0.000 07	−0.000 04	−0.014 98	−0.000 21	−0.015 19
Δf	−0.002 01	0.000 02	0.000 00		−0.001 99	−0.000 08	−0.002 07
Δg	−0.000 60				−0.000 60	−0.000 04	−0.000 64
Δh	−0.000 24				−0.000 24	−0.000 02	−0.000 26
ℓ tail	−0.000 27				−0.000 27	−0.000 09	−0.000 35
total	−109.923 33	−0.002 03	−0.000 07	−0.000 08	−109.925 50	0.012 51	−109.912 99
$2s2p\ ^1P_1$							
sp	−109.390 39	−0.001 39		−0.000 15	−109.391 93	0.012 74	−109.379 19
Δd	−0.050 48	−0.002 16	−0.000 55	−0.000 24	−0.053 43	−0.000 23	−0.053 66
Δf	−0.006 08	0.000 04	0.000 00		−0.006 04	−0.000 08	−0.006 12
Δg	−0.001 77				−0.001 77	−0.000 04	−0.001 81
Δh	−0.000 69				−0.000 69	−0.000 03	−0.000 72
ℓ tail	−0.000 72				−0.000 72	−0.000 09	−0.000 82
total	−109.450 13	−0.003 51	−0.000 55	−0.000 39	−109.454 58	0.012 26	−109.442 32

They are calculated with similar breakdowns as the Coulomb energies. But as corrections to the basic Breit energies are small ($<2\times10^{-5}$ a.u.), they are not shown separately here. The last column shows total no-pair energies which are given by the sum of the Coulomb and Breit energies. It should be noted that in actual calculations, Coulomb energies are calculated with the no-pair Hamiltonian restricted to the Coulomb interactions only, while no-pair energies are calculated with both the Coulomb and Breit interactions. Breit energies are given by the difference between the no-pair and Coulomb energies.

In Table I, results obtained with the s and p orbitals only are listed in the first rows under each state. Increments of energy by adding configurations with successive ℓ symmetries are shown in rows 2–5. Contributions from higher-ℓ states are obtained by extrapolations and are shown as ℓ tails in the sixth rows. Total multipole contributions are listed in the seventh rows.

For the $^{1,3}P_1$ states, we are unable to include all basic CSF's with $\ell=0$–5 in one CI expansion. However, tests show that high-ℓ contributions from the $1s2pn\ell n'\ell$ configurations are very small. As a result, it is sufficient to carry out basic CI calculations for the $^{1,3}P_1$ states with s, p, d, and f orbitals only. Incremental contributions to the basic Coulomb and Breit energies, Δg and Δh, are obtained by separate CI calculations with $\ell=0$–5 and with $1s2pn\ell n'\ell$ configurations omitted from the basic set of CSF's.

In full CI calculations that include all dominant CSF's from single, double, . . . excitations, results should be independent of the model potential used. That, in turn, provides important checks on the accuracy of these calculations. In Table II, alternative CI results are given for Ne^{6+}. They are similar to those shown in Table I, but are computed with a Dirac-Hartree (DH) potential for the He-like $1s^2$ ground state instead of the regular DS potential used here. Comparing results shown in these two tables, one sees that individual contributions to the Coulomb energy (basic, core-ch, $\Delta\ell\geqslant 2$, and triple) are strongly potential dependent and can differ by up to 1.5×10^{-3} a.u. However, when these terms are added up, total Coulomb and Breit energies indeed agree quite well, on a multipole by multipole basis, to within 2×10^{-5} a.u.

In Tables I and II, it can also be seen that all corrections to the Coulomb energies are the largest for the $^1P_1$ state. As a matter of fact, it does take a lot more effort to get converged results for this state. Furthermore, individual corrections are potential dependent and are consistently smaller when computed with the four-electron DS potential. This shows that it is possible to choose an optimal potential which minimizes contributions from small corrections such as triple excitations. That, in turn, allows the use of more compact basis sets to calculate these small corrections without compromising numerical accuracies. On the other hand, even though full CI results should be potential independent, poor choices like the point-Coulomb potential can lead to large corrections to the basic Coulomb and Breit energies and slow convergence of the CI results. The DS potential used here for the CI and QED calculations, though not necessarily an optimal choice, appears to work quite well.

In Table III, Coulomb, Breit, mass polarization, and QED

TABLE III. Coulomb, Breit, mass polarization (MP) and QED contributions to the total CI energies (a.u.) of the $2s^2\ ^1S_0$ and $2s2p\ ^{1,3}P_1$ states of Be-like ions.

Z	State	Coulomb	Breit	MP	QED	Total
10	$^1S_0$	−110.434 77	0.012 21	0.000 03	0.010 70	−110.411 83
	$^3P_1$	−109.925 49	0.012 52	−0.000 09	0.010 28	−109.902 78
	$^1P_1$	−109.454 57	0.012 27	−0.000 09	0.010 29	−109.432 10
15	$^1S_0$	−259.520 52	0.045 47	0.000 02	0.045 82	−259.429 21
	$^3P_1$	−258.664 53	0.047 05	−0.000 19	0.043 75	−258.573 92
	$^1P_1$	−257.880 98	0.045 94	−0.000 19	0.043 80	−257.791 43
20	$^1S_0$	−472.246 70	0.113 37	0.000 02	0.125 36	−472.007 95
	$^3P_1$	−471.016 85	0.117 90	−0.000 30	0.119 28	−470.779 97
	$^1P_1$	−469.878 53	0.114 46	−0.000 30	0.119 48	−469.644 89
26	$^1S_0$	−812.848 87	0.258 67	0.000 01	0.308 87	−812.281 32
	$^3P_1$	−811.117 24	0.271 02	−0.000 40	0.292 89	−810.553 73
	$^1P_1$	−809.406 00	0.260 37	−0.000 40	0.293 67	−808.852 36
32	$^1S_0$	−1248.6337	0.4955	0.0000	0.6245	−1247.5137
	$^3P_1$	−1246.3408	0.5222	−0.0005	0.5905	−1245.2286
	$^1P_1$	−1243.6957	0.4959	−0.0005	0.5928	−1242.6075
42	$^1S_0$	−2194.6996	1.1609	0.0000	1.5557	−2191.9830
	$^3P_1$	−2191.3709	1.2308	−0.0007	1.4655	−2188.6753
	$^1P_1$	−2185.4739	1.1518	−0.0007	1.4736	−2182.8491
54	$^1S_0$	−3716.8805	2.5625	0.0000	3.6048	−3710.7131
	$^3P_1$	−3712.1440	2.7249	−0.0009	3.3851	−3706.0349
	$^1P_1$	−3697.0622	2.5244	−0.0008	3.4076	−3691.1310
64	$^1S_0$	−5340.5216	4.4085	0.0000	6.3887	−5329.7244
	$^3P_1$	−5334.4042	4.6930	−0.0011	5.9878	−5323.7245
	$^1P_1$	−5304.0205	4.3182	−0.0010	6.0289	−5293.6744
74	$^1S_0$	−7330.1295	7.0686	0.0000	10.5015	−7312.5594
	$^3P_1$	−7322.3650	7.5324	−0.0013	9.8283	−7305.0056
	$^1P_1$	−7265.3327	6.8811	−0.0012	9.8913	−7248.5615
82	$^1S_0$	−9224.3511	9.9456	0.0001	15.0398	−9199.3657
	$^3P_1$	−9215.0393	10.6089	−0.0015	14.0641	−9190.3678
	$^1P_1$	−9124.3728	9.6290	−0.0013	14.1408	−9100.6043
90	$^1S_0$	−11 432.487	13.666	0.000	20.998	−11 397.823
	$^3P_1$	−11 421.492	14.595	−0.002	19.628	−11 387.271
	$^1P_1$	−11 281.170	13.149	−0.001	19.703	−11 248.320
92	$^1S_0$	−12 040.127	14.751	0.000	22.752	−12 002.624
	$^3P_1$	−12 028.707	15.760	−0.002	21.267	−11 991.682
	$^1P_1$	−11 872.707	14.170	−0.002	21.336	−11 837.202

contributions to the total energies of the $2s^2\ ^1S_0$ and $2s2p\ ^{1,3}P_1$ states are listed for 12 elements with $Z=10$–92. Here mass polarization corrections are calculated from first-order perturbation theory with the operator $H_{\mathrm{MP}}=(1/M)\Sigma_{i<j}\mathbf{p_i}\cdot\mathbf{p_j}$, where M is the nuclear mass, using eigenvectors from our CI calculations. Also, Coulomb energies shown here already include contributions from core angular momentum-changing corrections, along with those from $\Delta\ell\geqslant 2$ configurations and triple excitations. The latter two corrections are important for low-Z ions only. Specifically, corrections from triple excitations as computed with the DS potentials for the $^1S_0$ state are -0.000 019 a.u. at

TABLE IV. Theoretical and experimental ionization energies (a.u.) for the ground states of Be-like ions.

Z	Present work	FCPC [a]	Experiment
10	7.617 15	7.617 24	7.617 45[b]
15	20.608 87	20.608 95	20.608 67[c]
20	39.958 95	39.957 96	39.959 61[b]

[a] Chung, Zhu, and Wang, Ref. [16].

[b] Kelly, Ref. [33].

[c] Martin, Zalubas, and Musgrove, Ref. [34].

$Z=10$ and reduce to -0.000 003 a.u. at $Z=26$. For the $^3P_1$ and $^1P_1$ states, they are -0.000 033 and -0.000 239 a.u., respectively, at $Z=10$ and decrease to -0.000 005 and -0.000 023 a.u., respectively, at $Z=26$. Triple excitation contributions to the Breit interaction are entirely negligible. Similar trends hold for the $\Delta\ell\geqslant 2$ corrections.

Ionization energies from the present work for the $2s^2\ ^1S_0$ ground state are compared with results from the full-core plus correlation (FCPC) method [16] and with experiment [33,34] in Table IV. Our ionization energies are obtained by subtracting the Li-like $1s^22s$ energies given in Ref. [8] from corresponding Be-like $1s^22s^2$ energies shown in Table III. The only adjustment is that we have to exclude the $\Delta B(\omega)$ terms in the Li-like energies, as they are not calculated here. These are small corrections from the frequency-dependent Breit interaction to the off-diagonal CI matrix elements. They come mainly from the $1s^2$ core and are largely canceled between the Li-like $1s^22s$ and $1s^22p$ states. We expect the same to be true between the Li-like $1s^22s$ and Be-like $1s^22s^2$ states. As a result, leaving these $\Delta B(\omega)$ terms out should not affect the accuracy of our ionization energies here. The FCPC method uses the nonrelativistic multiconfiguration interaction approach and the effects of relativity are treated as first-order perturbations through the use of Breit-Pauli operators. For $Z=10$, 15, and 20, our results differ from FCPC by -0.000 09, -0.000 08, and 0.000 99 a.u., respectively. These discrepancies are due mainly to higher-order relativistic corrections. In general, agreements between theory and experiment are good for the ionization energies.

In Tables V and VI, theoretical and experimental x-ray energies for the $2s^2\ ^1S_0-2s2p\ ^3P_1$ and $^1P_1$ transitions are tabulated. Energies relative to the CI results and scaled by the atomic number Z are also plotted as functions of Z in Figs. 1 and 2. For low-Z ions, CI and FCPC [18] show good accord with experiment, while MBPT [23] deviates considerably from experiment. For mid-Z ions, CI, MBPT, and the all-order calculation [22] all agree with experiment. At high Z, CI and MBPT results are consistent with experiment for the $^1S_0-^1P_1$ transition.

For low-Z ions, discrepancies between theory and experiment are dominated by differences in correlation energies, while for high-Z ions, they are also affected by uncertainties in QED corrections. For $Z=92$, differences in correlation energies between the present CI and MBPT [23] are 0.03 and -0.39 eV for the $^1S_0-^3P_1$ and $^1P_1$ transitions, respectively, while differences in QED corrections are actually larger at 0.40 and 0.63 eV, respectively. These QED corrections are calculated with the same scheme [32] and their discrepancies are caused mostly by the use of different model potentials to account for electron screenings. In this work, we use four-electron DS potentials, while in Ref. [23], two-electron DH potentials are employed. This potential dependence in QED corrections is not likely to be resolved until higher-order QED calculations are carried out.

To make better comparisons between different correlation energy calculations, we show, in Figs. 3 and 4, theoretical energies without QED corrections for the $2s^2\ ^1S_0-2s2p\ ^3P_1$ and $^1P_1$ transitions. Results are relative to the MBPT energies [23] and scaled by Z. For the $^1S_0-^3P_1$ transition, these scaled energies are plotted as functions of 1/Z in Fig. 3. At low Z, CI, FCPC [18], and

TABLE V. Energies of the $2s2p\ ^3P_1$ state relative to the ground state in cm^{-1} for $Z=10-42$ and in eV for $Z=54-92$.

Z	CI	MBPT[a]	FCPC[b]	All-order[c]	Experiment	Reference
10	111 720	111 582	111 696		111 717(5)	[35]
					111 706	[36]
15	187 711	187 664			187 690	[34]
20	269 507	269 497			269 505(15)	[37]
26	379 158	379 102		379 118	379 140(20)	[38]
					379 130	[39]
32	501 535	501 449			501 605(75)	[40]
42	725 948	725 814		725 751	725 758(158)	[38]
54	127.301	127.267				
64	163.265					
74	205.549	205.598				
82	244.845					
90	287.150	287.511				
92	297.744	298.177				

[a] Safronova, Johnson, and Safronova, Ref. [23].

[b] Zhu and Chung, Ref. [18].

[c] Lindroth and Hvarfner, Ref. [22].

TABLE VI. Energies of the $2s2p\ ^1P_1$ state relative to the ground state in cm^{-1} for $Z=10$–42 and in eV for $Z=54$–92.

Z	CI	MBPT[a]	FCPC[b]	All-order[c]	Experiment	Reference
10	215 020	213 581	214 987		214 952(5)	[33]
15	359 445	358 537			359 343(13)	[34]
20	518 625	517 980			518 524(18)	[37]
26	752 562	752 015		752 459	752 372(57)	[38]
					752 502(120)	[39]
32	1 076 778	1 076 288			1 076 426(350)	[40]
42	2 004 633	2 004 151		2 004 464	2 003 847(1200)	[38]
54	532.854	532.759				
64	980.967					
74	1741.47	1741.37				
82	2687.43					
90	4068.19	4068.36			4068.47(16)	[2]
92	4501.36	4501.60			4501.72(27)	[1]

[a] Safronova, Johnson, and Safronova, Ref. [23].

[b] Zhu and Chung, Ref. [18].

[c] Lindroth and Hvarfner, Ref. [22].

MCDF [20] correlation energies agree quite well with each other, but are substantially larger than the MBPT results [23]. For high-Z ions, however, discrepancies between theories become very small.

More interesting comparisons between theories can be seen in Fig. 4, where the scaled, relative energies of the $^1S_0-{}^1P_1$ transition are shown as functions of Z in a log-log plot. Here CI and FCPC remain in good agreement at low Z, and show very similar systematic trends. Discrepancies of these two calculations with MCDF and MBPT, on the other hand, are substantially larger than those in the case of the $^1S_0-{}^3P_1$ transition throughout the isoelectronic sequence. Also, differences in energy between CI and MBPT show two distinct trends: At low Z, they scale roughly like $1/Z$, while, at high Z, they scale like Z^3 instead. This is consistent with analyses based on the Z-expansion theory. MBPT energies, which are carried out to second order in perturbation theory, should be exact to the Z^0 term in nonrelativistic $1/Z$ series expansions. As CI results are expected to be accurate to higher orders in these expansions, differences between the two calculations should be dominated by the $1/Z$ term at low Z. At high Z, relativistic corrections become more important, and these differences should scale as $(1/Z)(\alpha Z)^4$, or Z^3. Similar low-Z trend also exists in the case of the $^1S_0-{}^3P_1$ transition. But as differences in relativistic corrections are much smaller there, the high-Z trend shown in Fig. 3 is not as apparent as that shown in Fig. 4.

From these comparisons, it is clear that the FCPC method [16–18] can yield very accurate correlation energies for low-Z ions, but cannot extend to heavy systems due to the perturbative treatment of relativity. On the other hand, MBPT [23], including up to second-order corrections, works well for mid- to high-Z ions, but is not as satisfactory at low Z. MCDF results [20] are quite good for the $^1S_0-{}^3P_1$ transi-

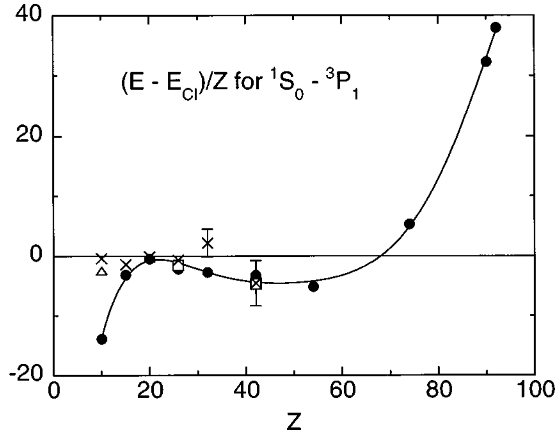

FIG. 1. The $2s^2\ ^1S_0-2s2p\ ^3P_1$ transition energies (cm^{-1}) relative to the present CI values are scaled by the atomic number Z and shown as functions of Z. Circles, triangles, and squares are MBPT [23], FCPC [18], and all-order [22] results, respectively. Crosses with error bars are experimental measurements.

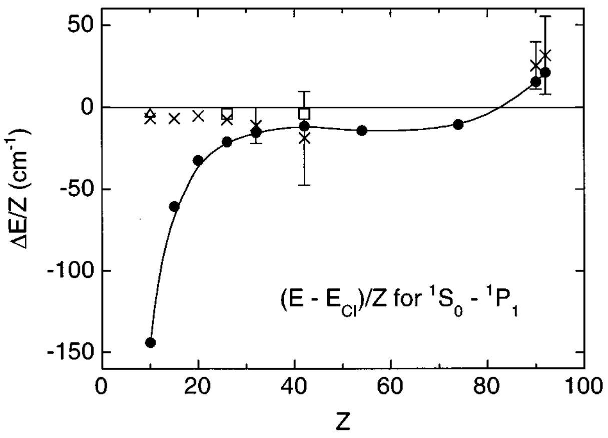

FIG. 2. The $2s^2\ ^1S_0-2s2p\ ^1P_1$ transition energies (cm^{-1}) relative to the present CI values are scaled by the atomic number Z and shown as functions of Z. Symbols are the same as those in Fig. 1.

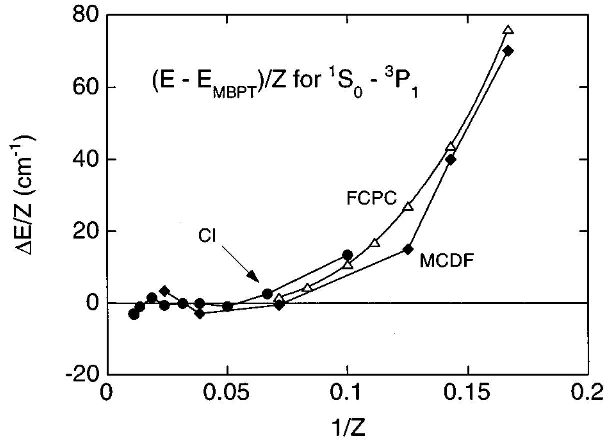

FIG. 3. Correlation energies (cm^{-1}) without QED corrections relative to the MBPT values [23] for the $2s^2\ {}^1S_0$–$2s2p\ {}^3P_1$ transition are scaled by the atomic number Z and shown as functions of $1/Z$. Circles, triangles, and diamonds are the present CI, FCPC [18], and MCDF [20] results, respectively.

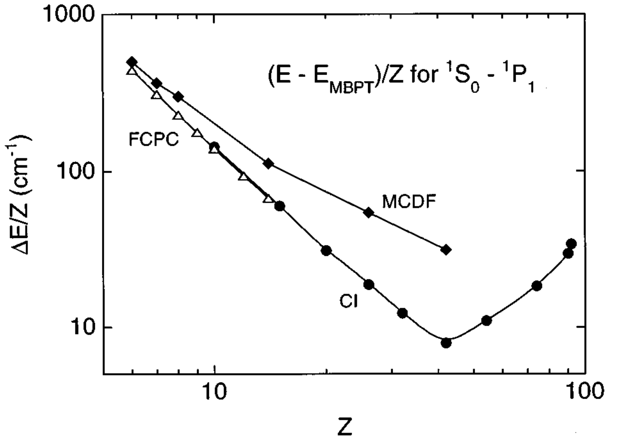

FIG. 4. Correlation energies (cm^{-1}) without QED corrections relative to the MBPT values [23] for the $2s^2\ {}^1S_0$–$2s2p\ {}^1P_1$ transition are scaled by the atomic number Z and shown as functions of Z. Symbols are the same as those in Fig. 3.

tion, but are not as accurate for the ${}^1S_0 - {}^1P_1$ transition. The all-order method [22] seems to work very well, but so far, results are available for Fe^{22+} and Mo^{38+} only. Our relativistic CI calculation appears to give accurate correlation energies for all the Be-like ions studied here. Even though our calculation starts from $Z = 10$, we expect that our method should work just as well for lower Z ions.

In summary we have calculated energy levels for the $2s^2\ {}^1S_0$ and $2s2p\ {}^{1,3}P_1$ states of Be-like ions with $Z = 10$–92 using the relativistic CI method with finite, B-spline basis functions. By including all dominant CSF's in the calculations, we have shown that our CI transition energy results are in very good agreement with experiment throughout the Periodic Table. The next stage of improvement in atomic structure calculations for heavy ions will depend on the advancement in the treatment of higher-order QED corrections. Also, corrections from nuclear polarizations [41], which can be of the same order of magnitude as residual discrepancies between theory and experiment for high-Z ions [9], may have to be addressed.

ACKNOWLEDGMENTS

We thank Professor K. T. Chung and Professor W. R. Johnson for helpful discussions and for communicating unpublished data. This work was performed under the auspices of the U.S. Department of Energy by Lawrence Livermore National Laboratory under Contract No. W-7405-ENG-48.

[1] P. Beiersdorfer, D. Knapp, R. E. Marrs, S. R. Elliot, and M. H. Chen, Phys. Rev. Lett. **71**, 3939 (1993).
[2] P. Beiersdorfer, A. Osterheld, S. R. Elliott, M. H. Chen, D. Knapp, and K. Reed, Phys. Rev. A **52**, 2693 (1995).
[3] J. F. Seely, U. Feldman, C. M. Brown, M. C. Richardson, D. D. Dietrich, and W. E. Behring, J. Opt. Soc. Am. B **5**, 785 (1988).
[4] J. F. Seely, C. M. Brown, U. Feldman, J. O. Ekberg, C. J. Keane, B. J. MacGowan, D. R. Kania, and W. E. Behring, At. Data Nucl. Data Tables **47**, 1 (1991).
[5] D. D. Dietrich, A. Simionovici, M. H. Chen, G. Chandler, C. J. Hailey, P. O. Egan, P. H. Mokler, S. Reusch, and D. H. H. Hoffmann, Phys. Rev. A **41**, 1450 (1990).
[6] M. H. Chen, K. T. Cheng, and W. R. Johnson, Phys. Rev. A **47**, 3692 (1993).
[7] K. T. Cheng, M. H. Chen, W. R. Johnson, and J. Sapirstein, Phys. Rev. A **50**, 247 (1994).
[8] M. H. Chen, K. T. Cheng, W. R. Johnson, and J. Sapirstein, Phys. Rev. A **52**, 266 (1995).
[9] K. T. Cheng and M. H. Chen, Phys. Rev. A **53**, 2206 (1996).
[10] W. R. Johnson, S. A. Blundell, and J. Sapirstein, Phys. Rev. A **37**, 2764 (1988); **38**, 2699 (1988); **42**, 1087 (1990).
[11] W. R. Johnson and J. Sapirstein, Phys. Rev. A **46**, R2197 (1992).
[12] D. R. Plante, W. R. Johnson, and J. Sapirstein, Phys. Rev. A **49**, 3519 (1994).
[13] W. R. Johnson, J. Sapirstein, and K. T. Cheng, Phys. Rev. A. **51**, 297 (1995).
[14] E. P. Ivanova and U. I. Safronova, J. Phys. B **8**, 1591 (1975).
[15] K. Ando, U. I. Safronova, and I. Y. Tolstikhiva, Phys. Scr. **46**, 107 (1992).
[16] K. T. Chung, X.-W. Zhu, and Z.-W. Wang, Phys. Rev. A **47**, 1740 (1993).
[17] K. T. Chung and X.-W. Zhu, Phys. Rev. A **48**, 1944 (1993).
[18] X.-W. Zhu and K. T. Chung, Phys. Rev. A **50**, 3818 (1994).
[19] K. T. Cheng, Y. K. Kim, and J. P. Desclaux, At. Data Nucl. Data Tables **24**, 111 (1979).
[20] A. Ynnerman and C. Froese Fischer, Phys. Rev. A **51**, 2020 (1995).
[21] Z. W. Liu and H. P. Kelley, Phys. Rev. A **43**, 3305 (1991).
[22] E. Lindroth and J. Hvarfner, Phys. Rev. A **45**, 2771 (1992).
[23] M. S. Safronova, W. R. Johnson, and U. I. Safronova, Phys. Rev. A **53**, 4036 (1996).

[24] J. Sucher, Phys. Rev. A **22**, 348 (1980).

[25] M. H. Mittleman, Phys. Rev. A **4**, 893 (1971); **5**, 2395 (1972); **24**, 1167 (1981).

[26] W. R. Johnson, S. A. Blundell, and J. Sapirstein, Phys. Rev. A **37**, 307 (1988).

[27] W. R. Johnson and G. Soff, At. Data Nucl. Data Tables **33**, 405 (1985).

[28] J. D. Zumbro, R. A. Naumann, M. V. Hoehn, W. Reuter, E. B. Shera, C. E. Bemis, Jr., and Y. Tanaka, Phys. Lett. **167B**, 383 (1986).

[29] J. D. Zumbro, E. B. Shera, Y. Tanaka, C. E. Bemis, Jr., R. A. Naumann, M. V. Hoehn, W. Reuter, and R. M. Steffen, Phys. Rev. Lett. **53**, 1888 (1984).

[30] E. R. Davidson, J. Comput. Phys. **17**, 87 (1975).

[31] A. Stathopoulos and C. Froese Fischer, Comput. Phys. Commun. **79**, 268 (1994).

[32] K. T. Cheng, W. R. Johnson, and J. Sapirstein, Phys. Rev. A **47**, 1817 (1993); Phys. Rev. Lett. **66**, 2960 (1991).

[33] R. L. Kelly, J. Phys. Chem. Ref. Data **16**, Suppl. 1 (1987).

[34] W. C. Martin, R. Zalubas, and A. Musgrove, J. Phys. Chem. Ref. Data **14**, 751 (1985).

[35] B. Edlén, Phys. Scr. **28**, 51 (1983).

[36] S. Baskin and J. O. Stoner, Jr., *Atomic Energy Level and Grotrian Diagrams II* (Elsevier, New York, 1975).

[37] J. Sugar and C. Corliss, J. Phys. Chem. Ref. Data **14**, Suppl. 2 (1985).

[38] B. Denne, G. Magyar, and J. Jacquinot, Phys. Rev. A **40**, 3702 (1989).

[39] T. Shirai, Y. Funatake, K. Mori, J. Sugar, W. L. Wiese, and Y. Nakai, J. Phys. Chem. Ref. Data **19**, 127 (1990).

[40] J. Sugar and A. Musgrove, J. Phys. Chem. Ref. Data **22**, 1213 (1993).

[41] G. Plunien and G. Soff, Phys. Rev. A **51**, 1119 (1995); **53**, 4614 (1996).